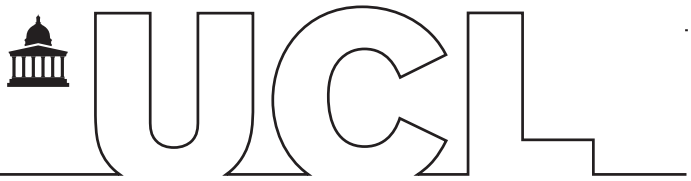

University College London

UCL PhD Upgrade Report

Qubit Coherence and Control

Author:
David F. Wise

Supervisor:
Prof. John Morton

Submitted in partial fulfilment for the degree of MRes Quantum Technologies

February 26, 2018

Abstract

Scientific documents often use LaTeX for typesetting. While numerous packages and templates exist, it makes sense to create a new one. Just because.

Contents

1 Introduction 1

2 Theory 5
2.1 Electron Spin Resonance 5
2.1.1 Background Theory 5
2.1.2 Pulsed Electron Spin Resonance and Qubits 6
2.2 Donor States in Silicon 7
2.2.1 The Hyperfine interaction 7
2.2.2 Spin Transitions 8
2.2.3 Relaxation Processes 10

List of Figures

2.1 Free electron level splitting 5
2.2 Hahn echo sequence 7
2.3 Bloch Sphere 8
2.4 Phosphorus energy levels and transitions 9

1 Introduction

At midnight all the agents and
superhuman crew come out and round up
everyone that knows more than they do

Quantum computing has been an active field of research since the concept was first suggested by Richard Feynman in the early 1980s [7]. Originally proposed as an efficient method for simulating chemical processes (something that traditional computers find extremely taxing) the discovery of several algorithms offering significant speed increases over classical computers has further fueLled research [19, 20]. Strong initial scepticism abounded regarding the potential for quantum computers to exist in the real world, primarily due to the concerns that error correction with such a complex device would be impossible[15]. This pessimism gave way with the identification of an error threshold for quantum computation. Given an error rate below a critical threshold it was possible to perform an arbitrarily long computation with negligible possibility of significant error [1, 18]. Following these discoveries serious attention has been given to the development of error correcting codes that might be implemented to allow a physical quantum computer to be *fault tolerant*.

Gottesman identified the class of error correcting codes known as *stabilizer codes*, where codes are defined by the group of logical operators that leave the code unchanged [8]. This class of quantum error correcting codes have become the dominant form in theoretical research. Of these one in particular has become the focus of much of the ongoing research of quantum computing, *the surface code*, developed by Bravyi and Kitaev [4]. Although other quantum error correcting codes (such as colour codes [21]) exist, the surface code has become the focus for experimental implementations. This is due mainly to the relatively high error threshold that it is able to tolerate, $\sim 0.5\%$, and the simple architecture of a planar grid of qubits.

In recent years there has been rapid progress in the development of physical qubits. Groups in both the academic and private sectors have shown small numbers of qubits functioning with error rates above the fault tolerant threshold [3, 16]. The successful recent approaches have tended to focus on superconducting circuits to produce their qubits. Whilst these have proved excellent for the small numbers of qubits currently in use, it is likely that they will present significant

additional challenges when scaling to numbers sufficient for useful, fault-tolerant quantum computation. With the numbers required likely to be close to 100×10^6 and the current size of these qubits close to 1mm^2, it will likely be impossible to use these qubits in their current form in a fault-tolerant quantum computer.
Although there are many alternative systems that could provide a qubit, this paper will focus on the use of the spins of nuclei and electrons bound to donors in semiconductors, particularly silicon. A seminal paper by Kane [10] stimulated much of the research interest in this field. He proposed using the spin of phosphorus nuclei in silicon as qubits with the ability to mediate interactions between neighbouring donor nuclei using the interaction between the electrons bound to each. These types of qubit are attractive due to their exceptionally long coherence times, the time that the qubit reliably stores quantum information for. A long coherence time relative to qubit gate times is essential, as this determines the error rate of the qubits. Coherence times as long as several seconds have been reported for donor spin qubits in silicon, whilst gate times can be as low as several nanoseconds [22]. Despite these advantages, development of these types of qubits for quantum computers has lagged behind the superconducting and ion trap versions [2]. This is due to the difficulty of isolating and addressing single donors in a silicon lattice. Kane's proposal required sub nano-metre precision in qubit placement to facilitate inter-qubit interactions. Even if this precision were achieved there remains the issue of how the requisite control circuitry could be integrated into such a dense design. This has lead to the development of more modern proposals to both overcome these difficulties and also to implement surface code based error correction.

One such proposal is from O'Gormann et al [13]. This proposal takes a similar approach to Kane, with qubits being donor spins in a silicon lattice. Where it differs significantly is in its use of two lattices of qubits. One of these is for the storage of data, whilst the other performs measurements on these data qubits. This measurement stage is placed above the data stage and held close, within 40nm, and moved in a repeating cycle over the data qubits. This allows each measurement qubit to perform $\hat{X}$ or $\hat{Z}$ measurement on groups of four data qubits, the stabilizer measurements that make up the fundamental units of surface code. This architecture allows for data qubits to be placed much farther apart - since no direct interaction between them is required. Several key research questions remain:

1. What donor species should be used for both types of qubit?

2. How are the measurement qubits to be read out?

3. How are the qubits to be controlled?

Whilst donors in silicon make excellent choices for the data qubits due to the properties stated above, a different qubit species is required for the measurement qubits to avoid an unwanted exchange interaction between the two lattices. Optical qubit readout is suggested in the proposal by O'Gormann et al and is a well studied means of reading the state of spin qubits, particularly in nitrogen-vacancy (NV) centres in diamond [11]. A concern with optical readout is the impact that illumination can have on the coherence times of donors in silicon. Silicon has a band gap energy equivalent to approximately 1058nm or photon energy of 1.17eV. Illumination at shorter wavelengths than this will create free electrons in the silicon conduction band. These can scatter off the electrons bound to donors, causing them to relax and shortening the T_1 time of the qubits as a whole [17]. NV centres are read out at between 500nm and 600nm, illumination that would reduce data qubit coherence times and increase the qubit error rate. Alternative optically addressed spin qubits at higher wavelengths exist, such as the di-vacancy centre in silicon carbide [5], but a vital question is what wavelengths can be used for read-out without compromising data qubit coherence times. This report addresses this question by examining the effect of various laser wavelengths close to the silicon band gap on the coherence times of electrons bound to phosphorus donors in silicon.

Another key question presented by the O'Gormann proposal is how to control the data qubits. The frequencies traditionally used for electron spin resonance are between 8GHz and 10GHz. Electromagnetic radiation at these frequencies require large coaxial cables and cavities for transmission. This makes it almost impossible to individually address qubits using microwaves. Instead the solution proposed by Kane is to use global microwave pulses, addressing all qubits at once. To selectively control qubits the DC Stark shift can be employed - DC electric fields can be used to shift the electron spin transition frequency meaning that a global microwave field will not effect them. Unlike RF radiation, DC signals are easily multiplexed and the commercial electronics industry has achieved fabrication precision well within that required by the O'Gormann proposal. The stark shift of donors in silicon has been well studied but has yet to be quantified in certain systems [14]. Among these is the hyperfine interaction between the donor electron and the silicon-29 nuclei present in natural silicon. The nuclear bath has been identified as a potential quantum register and the ability to tune the interaction between data qubits and memory could be of use.

2 Theory

2.1 Electron Spin Resonance

2.1.1 Background Theory

Electron spin resonance (EPR) functions by detecting the energy difference between the spin states of an electron. Normally degenerate, the presence of a magnetic field separates the two spin states parallel to it in energy - known as the Zeeman splitting [6]. The spin state parallel to the magnetic field has a lower energy whilst the anti-parallel state has a higher energy. These are described as the up, $|\uparrow\rangle$, and down, $|\downarrow\rangle$, spin states. For an electron in free space the energy difference is given by:

$$\Delta E = g_e \mu_b B, \tag{2.1}$$

where g_e is the free electron g-factor, μ_b is the Bohr magneton and $B$is the magnetic field strength. This results in an energy splitting as seen in figure 2.1.

In practice this energy splitting can be detected using continuous wave EPR. Transitions between the spin states will be driven by incident electromagnetic radiation of photon energy equal to the energy gap (i.e $h\nu = g_e \mu_b B$). The presence of an EPR transition in a sample can be detected either by applying a constant magnetic field and sweeping EM frequency incident on that

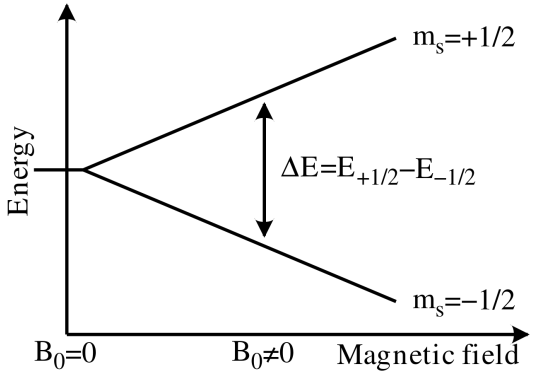

Figure 2.1: Spin state energy splitting for a free electron in a magnetic field.

sample or vice versa. In practice, it is the latter that is used for experimental simplicity. Measuring reflection of radiation from the sample whilst sweeping magnetic field will reveal a drop in reflection at the transition field - when photons are absorbed by spins moving from the lower to higher energy state.

2.1.2 Pulsed Electron Spin Resonance and Qubits

The description above details continuous wave (CW) ESR, a technique that has proven invaluable for studying the electronic structure of materials. Another ESR has proven more popular for the manipulation of spins for use of qubits: pulsed ESR. This uses short bursts of microwave radiation, on resonance with the spin transition, to control spin states and allows the spin to function as a qubit. This control is achieved by placing the spins at the centre of a cavity which produces a magnetic field when a pulse is applied. This magnetic field causes precession which can be used to rotate the spins. Pulses are described in terms of a rotation angle, with a π pulse taking the ensemble of spins from the down to up state or vice versa. A $\pi/2$ pulse takes the spins into the plane normal to the magnetic field, termed the $x-y$ plane. This causes the spins to precess in the static magnetic field at the Lamor frequency given by:

$$\omega = \frac{eg}{2m} B_0 \tag{2.2}$$

Hahn Echo and Detection

In pulsed ESR the spins are detected via the electromagnetic radiation they emit when precessing in a magnetic field. This radiation is of the same frequency as the resonant control radiation (easily shown using equations 2.1 and 2.2). This emitted radiation can be demodulated with the control radiation giving a DC signal. In a perfectly homogeneous magnetic field all spins would precess at the same rate giving a constant DC signal. In reality however, all spins will precess at slightly different rates due to small, static differences in the magnetic field each experiences. So, following a $\pi/2$ pulse, the signal from the spins will rapidly decay as the ensemble of spins lose phase coherence. A technique, known as a spin or Hahn echo, to reverse this loss of phase was developed by Erwin Hahn in 1950 [9]. This follows a $\pi/2$ pulse with a π pulse after a set time interval, T. *Static* magnetic field differences now act to reverse the loss of phase coherence. This results in a brief re-phasing of the spins following another interval T, detected as a rise and fall of a DC signal or and 'Echo'. A cartoon of this sequence is shown in figure 2.2.

The Bloch Sphere

The control pulses produce a magnetic field that rotates at the same rate as the spins, meaning a fixed coordinate system can be defined. The rotation axis of the control pulses can be changed by

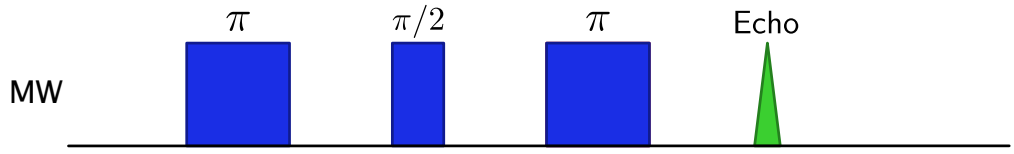

Figure 2.2: Cartoon showing a Hahn echo pulse sequence. A $\frac{\pi}{2}$ pulse causes the spins to precess in the $x-y$ plane. Loss of phase coherence is reversed via a π pulse following time interval T and a signal is detected following another interval of T.

varying their phase, for example to a pulse of 0 phase is defined as a rotation about the x axis whilst a pulse of $\pi/2$ phase is a rotation about the y. This allows control of the direction of the spin vector in 3-D space, with the z-axis defined by the static magnetic field. A qubit, the basic unit of a quantum computer, can be described as a point within a unit sphere, known as a Bloch sphere and shown in figure 2.3 [12]. Clearly then, a single spin is an archetypal qubit: its eigenstates of $|\uparrow\rangle$ and $|\downarrow\rangle$ form the poles of the Bloch sphere. Microwave pulses of defined duration and phase enable the creation of an arbitrary linear superposition that allows the initialisation of any state on the surface of the Bloch sphere. In the case of ESR, however, a huge number (10^{10}) of spins is being addressed. Although this means that they do not represent a true qubit, measurements of ensemble properties give great insight into the behaviour of single spins. It is therefore prudent to establish the anticipated behaviour of the various potential spin qubit candidates using the comparatively simple experimental techniques of ESR before making the challenging step to single spin control and measurement.

2.2 Donor States in Silicon

2.2.1 The Hyperfine interaction

Discussion so far has focussed on single electrons in a magnetic field. The spins discussed in this thesis will be those of the electrons and nuclei of donors in silicon. For these spin states the situation is a little more complicated than the case of a free electron. For all the donors discussed here, there is a nuclear as well as electron spin. This introduces first an additional term in the Hamiltonian of the system due to the nuclear spin's Zeeman interaction with the magnetic field. On top of the separate Zeeman interactions there is an additional interaction between the nucleus and the electron, known as the hyperfine interaction. This term is due to the magnetic field of the electron interacting with the magnetic dipole moment of the nucleus. This strength of this interaction is proportional to the overlap between the electron and nuclear wavefunctions. The result of this is that it is preferential energetically for the electron and nuclear spins to be anti-aligned. A further

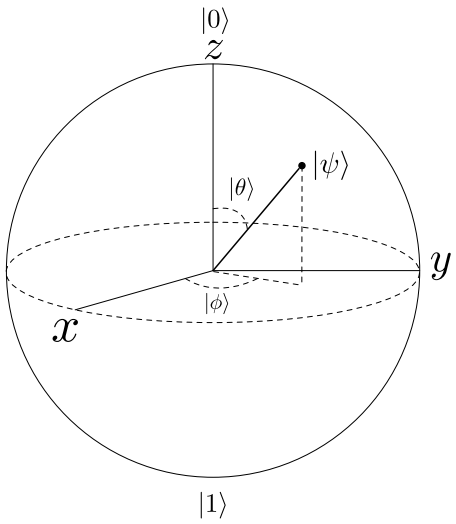

Figure 2.3: Diagram of the Bloch sphere - the most common representation of a qubit. The poles of the sphere at $\pm z$ represent the $|0\rangle$ and $|1\rangle$ or $|\uparrow\rangle$ and $|\downarrow\rangle$ states. Any point on the surface of the sphere represents some linear superposition of these two states. The state vector of any point is given by: $|\psi\rangle = \cos\theta/2\,|0\rangle + e^{i\phi}\sin\theta/2\,|1\rangle$

term in the Hamiltonian is due to the nuclear quadrupole but this effect is small enough to be neglected in this treatment. These effects leave a Hamiltonian of the following form:

$$\hat{H} = \mu_b g_e B_0 \hat{S}_z + \mu_n g_n B_0 \hat{I}_z + A\hat{S}\cdot\hat{I}, \tag{2.3}$$

where μ_b&μ_n are the Bohr and nuclear magnetons, g_e&g_n are the electron and nuclear g-factors, $\hat{S}$&$\hat{I}$ are the electron and nuclear spin operators, and A is the hyperfine interaction term. In general they hyperfine term is a tensor but due to the isotropic nature of silicon can be represented as a scalar here.

2.2.2 Spin Transitions

The electron spin is restricted to be $\pm\frac{1}{2}$, but the nuclear spin can take a much greater range of values. The nuclear spin of a phosphorus donor in silicon is $\pm\frac{1}{2}$, by contrast for a bismuth spin it can take the values $-\frac{9}{2}, -\frac{7}{2}, ...\frac{7}{2}, \frac{9}{2}$. In the simple case of phosphorus this results in the four energy levels seen in figure 2.4.

For the more complex case of bismuth, instead of 4 possible energy levels there are 20. Not all transitions are possible - spins are changed by the absorption or emission of a photon, leaving only transitions where the total spin changes by ± 1 as allowed. This means that only nuclear or

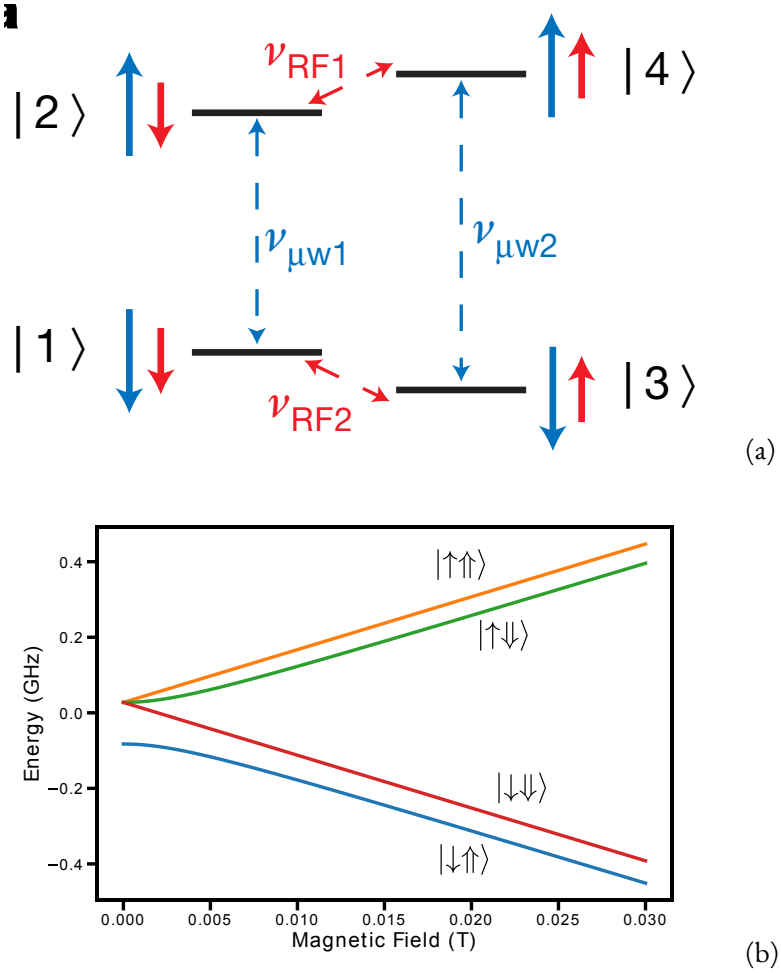

Figure 2.4: Cartoon in a shows the relative energy levels for the different spin states of phosphorus in a high field environment. Note that in this case the electron Zeeman interaction dominates the hyperfine term which dominates the nuclear Zeeman term. b shows the simulated energies for each of the four possible states of the system.

electron spin can be flipped at once, not both. It should be clear that the transitions that involve an electron spin flip (e.g. $|\uparrow\Uparrow\rangle \longrightarrow |\downarrow\Uparrow\rangle$) are significantly higher in energy than those involving a nuclear spin flip (e.g. $|\uparrow\Uparrow\rangle \longrightarrow |\uparrow\Downarrow\rangle$). At typical experimental magnetic fields ($\approx$ 0.3 Tesla), the nuclear transitions are at frequencies of 10s of MHz, whilst the electron transitions are at $\approx$ 9.7 GHz. In addition to their different energies electron and nuclear transitions have different strengths or Rabi frequencies. The electron spin transition is much stronger and occurs on the order of nanoseconds at typical pulse powers, with the nuclear transition being on the order of microseconds.

2.2.3 Relaxation Processes

For spins in silicon, three main relaxation or decoherence processes occur, causing the loss of information.

Dephasing

The first of these was briefly discussed above - dephasing - the time scale for the process is termed T_2^* This is the process by which an ensemble of spins loses phase coherence due to each spin experiencing a different static magnetic field. As was described above, this loss of information can be reversed by a Hahn echo sequence.

Relaxation

The second process is known as relaxation and its time scale is termed T_1. A spin ensemble at a given temperature and magnetic field will have a Boltzmann distributed population across the available spin states defined by the magnetic field axis (i.e. across the eigenstates of the $\hat{Z}$ operator). The difference between higher and lower energy states is known as the polarisation of the ensemble. If this polarisation is reversed by a π pulse, then on a time scale T_1 it will relax back to thermal equilibrium. This process is strongly correlated with temperature and exact mechanisms will be discussed in the literature review section.

Decoherence

The third process, decoherence, occurs on the time scale T_2. This is similar to the dephasing process described above but is irreversible. Irreversible phase differences are caused by by inhomogeneous and *time dependend* magnetic fields. Additional phase acquired due to a time varying magnetic field will not be reversed by a Hahn echo sequence as the field will act differently on the spin in the second half of the sequence.

Bibliography

1. D. Aharonov and M. Ben-Or. "Fault-tolerant quantum computation with constant error". *Proceedings of the twenty-ninth annual ACM symposium on Theory of computing - STOC '97*, 1997, pp. 176–188. ISSN: 1533-. DOI: 10.1145/258533.258579. arXiv: 9906129v1 [arXiv:quant-ph].
2. C. J. Ballance et al. "Laser-driven quantum logic gates with precision beyond the fault-tolerant threshold". *arXiv preprint*, 2015, pp. 1–12. arXiv: 1512.04600. URL: http://arxiv.org/abs/1512.04600.
3. R. Barends et al. "Digital quantum simulation of fermionic models with a superconducting circuit". *Nature Communications* 6:May, 2015, p. 7654. ISSN: 2041-1723. DOI: 10.1038/ncomms8654. arXiv: 1501.07703v1. URL: http://www.nature.com/ncomms/2015/150708/ncomms8654/full/ncomms8654.html{\%}5Cnhttp://www.nature.com/doifinder/10.1038/ncomms8654.
4. S. B. Bravyi and A. Y. Kitaev. "Quantum codes on a lattice with boundary . *". 96, 2008, pp. 1–6. arXiv: 9811052v1 [arXiv:quant-ph].
5. D. J. Christle et al. "Isolated electron spins in silicon carbide with millisecond coherence times". *Nature Materials* 14:2, 2014, pp. 160–163. ISSN: 1476-1122. DOI: 10.1038/nmat4144. arXiv: 1406.7325. URL: http://www.nature.com/doifinder/10.1038/nmat4144.
6. G. Feher. "Electron spin resonance experiments on donors in silicon. I. Electronic structure of donors by the electron nuclear double resonance technique". *Physical Review* 114:5, 1959, pp. 1219–1244. ISSN: 0031899X. DOI: 10.1103/PhysRev.114.1219.
7. R. P. Feynman. "Simulating physics with computers". *International Journal of Theoretical Physics* 21:6-7, 1982, pp. 467–488. ISSN: 00207748. DOI: 10.1007/BF02650179. arXiv: 9508027 [quant-ph].
8. D. Gottesman. "Stabilizer Codes and Quantum Error Correction". 2008, 1997. ISSN: 0163-6804. DOI: 10.1017/CBO9781107415324.004. arXiv: 9705052 [quant-ph].
9. E. L. Hahn. "Spin Echoes". *Physical Review* 80:4, 1950, pp. 580–594.
10. B. E. Kane. "A silicon-based nuclear spin quantum computer". *Nature* 393:6681, 1998, pp. 133–137. ISSN: 0028-0836. DOI: 10.1038/30156. URL: http://www.nature.com/doifinder/10.1038/30156{\%}5Cnpapers2://publication/doi/10.1038/30156.
11. G. Q. Liu et al. "Single-Shot Readout of a Nuclear Spin Weakly Coupled to a Nitrogen-Vacancy Center at Room Temperature". *Physical Review Letters* 118:15, 2017, pp. 1–5. ISSN: 10797114. DOI: 10.1103/PhysRevLett.118.150504. arXiv: 1612.07944.

12. M. A. Nielsen and I. L. Chuang. *Quantum Computation and Quantum Information: 10th Anniversary Edition*. 10th. Cambridge University Press, New York, NY, USA, 2011. ISBN: 1107002176, 9781107002173.

13. J. O'Gorman et al. "A silicon-based surface code quantum computer". *arXiv* 1:October 2015, 2014, pp. 1–11. ISSN: 2056-6387. DOI: 10.1038/npjqi.2015.19. arXiv: 1406.5149.

14. G. Pica et al. "Hyperfine Stark effect of shallow donors in silicon". *Physical Review B - Condensed Matter and Materials Physics* 90:19, 2014, pp. 1–10. ISSN: 1550235X. DOI: 10.1103/PhysRevB.90.195204. arXiv: 1408.4375v1.

15. J. Preskill. "Reliable Quantum Computers", 1997, pp. 1–24. ISSN: 1364-5021. DOI: 10.1098/rspa.1998.0167. arXiv: 9705031 [quant-ph]. URL: http://arxiv.org/abs/quant-ph/9705031{\%}0Ahttp://dx.doi.org/10.1098/rspa.1998.0167.

16. M. Reagor et al. "Demonstration of Universal Parametric Entangling Gates on a Multi-Qubit Lattice", 2017, pp. 1–7. arXiv: 1706.06570. URL: http://arxiv.org/abs/1706.06570.

17. M. P. Ross. "Bound exciton-assisted spin-to-charge conversion of donors in silicon". PhD thesis. 2017.

18. P. W. Shor. "Fault-tolerant quantum computation", 1996. ISSN: 0272-5428. DOI: 10.1109/SFCS.1996.548464. arXiv: 9605011 [quant-ph]. URL: http://arxiv.org/abs/quant-ph/9605011.

19. P. W. Shor. "Polynomial-Time Algorithms for Prime Factorization and Discrete Logarithms on a Quantum Computer*". *SIAM Journal on Computing* 26:5, 1997, pp. 1484–1509. ISSN: 0097-5397. DOI: 10.1137/S0097539795293172. arXiv: 9508027 [quant-ph].

20. P. Shor. "Algorithms for quantum computation: discrete logarithms and factoring". *Proceedings 35th Annual Symposium on Foundations of Computer Science*, 1994, pp. 124–134. ISSN: 0272-5428. DOI: 10.1109/SFCS.1994.365700.

21. M. Vasmer and D. E. Browne. "Universal Quantum Computing with 3D Surface Codes", 2018, pp. 1–21. arXiv: 1801.04255. URL: http://arxiv.org/abs/1801.04255.

22. G. Wolfowicz et al. "Atomic clock transitions in silicon-based spin qubits." *Nature nanotechnology* 8:8, 2013, pp. 561–4. ISSN: 1748-3395. DOI: 10.1038/nnano.2013.117. arXiv: 1301.6567. URL: http://www.ncbi.nlm.nih.gov/pubmed/23793304.